## Calculation of Diffraction Coefficients of Three-Dimensional Infinite Conducting Wedges Using FDTD

Veeraraghavan Anantha and Allen Taflove

Abstract—The finite-difference time-domain (FDTD) method is applied to obtain the three-dimensional (3-D) dyadic diffraction coefficient of infinite right-angle perfect electrical conductor (PEC) wedges illuminated by a plane wave. The FDTD results are in good agreement with the well-known asymptotic solutions obtained using the uniform theory of diffraction (UTD). In principle, this method can be extended to calculate diffraction coefficients for 3-D infinite material wedges having a variety of wedge angles and compositions.

Index Terms—Electromagnetic scattering, FDTD methods.

We extend the two-dimensional (2-D) approach discussed in [1] to obtain numerically the three-dimensional (3-D) dyadic diffraction coefficients for right-angle perfect electrical conductor (PEC) wedges. This method exploits the temporal causality inherent in finite-difference time-domain (FDTD) modeling. In principle, this method can be extended to calculate diffraction coefficients for 3-D infinite material wedges having a variety of wedge angles and compositions.

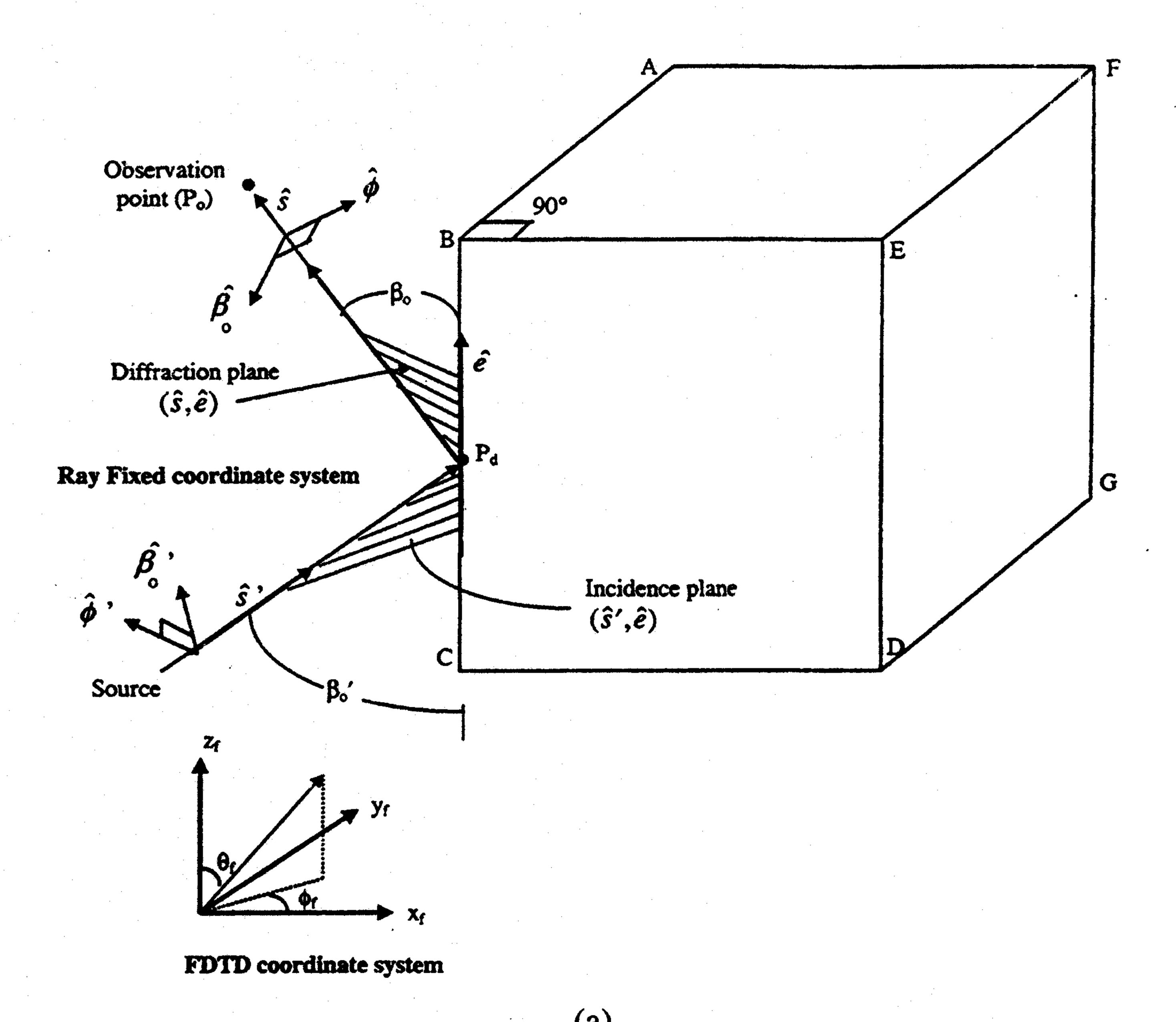
Diffraction from a PEC wedge illuminated by an obliquely incident plane wave can be described by a dyadic diffraction coefficient [2]. By choosing the appropriate ray-fixed coordinates [Fig. 1(a) and (b)], the diffraction coefficient is described as a sum of two dyads [2], which, in matrix notation, is represented by a diagonal  $2 \times 2$  matrix. The two nonvanishing elements are the soft and the hard scalar diffraction coefficients  $D_s$  and  $D_h$ . Fig. 1(a) shows the edge-fixed plane of incidence  $(\hat{s}', \hat{e})$  with the ray-fixed unit vectors  $\hat{\beta}'_0$  and  $\hat{\phi}'$  parallel and perpendicular to it, respectively. Also shown is the edge-fixed

Manuscript received March 20, 1998; revised July 21, 1998.

V. Anantha is with the Cellular Infrastructure Group, Motorola Inc., Arlington Heights, IL 60004 USA.

A. Taflove is with the Department of Electrical and Computer Engineering, Northwestern University, Evanston, IL 60208 USA.

Publisher Item Identifier S 0018-926X(98)08903-0.



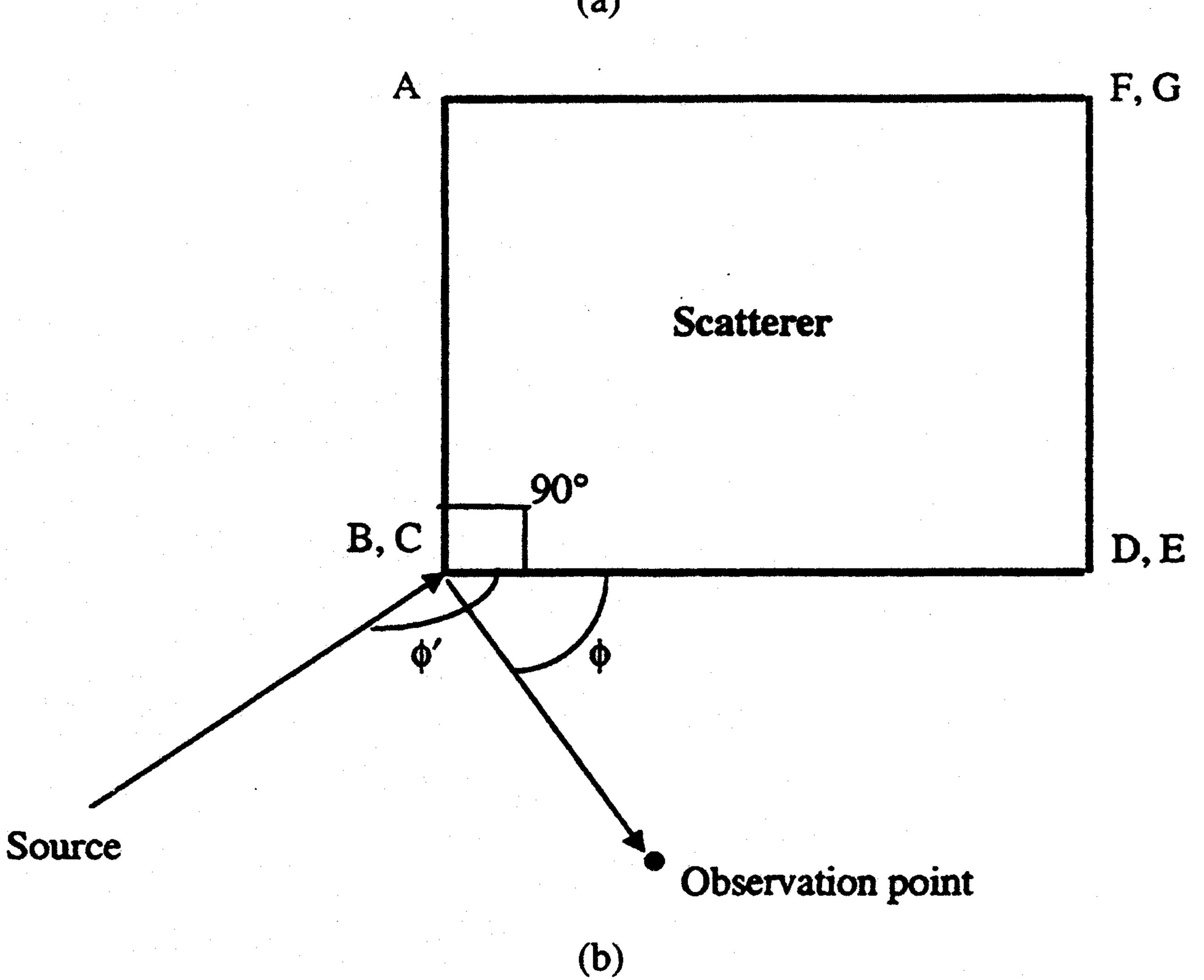


Fig. 1. (a) Three-dimensional geometry of the PEC scatterer showing the edge-fixed plane of incidence and diffraction, the ray-fixed coordinate system, and the FDTD coordinate system. (b) Top view of the scattering edge showing the angles made by the projections of the incident and diffracted wavevectors in plane ABEF.

plane of diffraction  $(\hat{s}, \hat{e})$  with the ray-fixed unit vectors  $\hat{\beta}_0$  and  $\hat{\phi}$  parallel and perpendicular to it, respectively. The radial unit vectors of incidence and diffraction are given by  $\hat{s}' = \hat{\phi}' \times \hat{\beta}'_0$  and  $\hat{s} = \hat{\phi} \times \hat{\beta}_0$ .

In order to obtain the numerical dyadic diffraction coefficient, we first find the diffracted-field impulse response of the scatterer numerically using FDTD. By illuminating the wedge with a pulsed plane wave having an electric field (E-field) component parallel to the plane of incidence, we obtain the diffracted-field impulse response  $h_{\beta_0,\text{num}}$  polarized parallel to the plane of diffraction. An analogous procedure is performed with the incident E-field component perpendicular to the plane of incidence, yielding  $h_{\phi,\text{num}}$  polarized perpendicular to the plane of diffraction. The Fourier transforms of these diffracted-field impulse responses  $H_{\beta_0,\text{num}}$  and  $H_{\phi,\text{num}}$ , give the corresponding spectra of the diffracted fields.  $D_s$ 

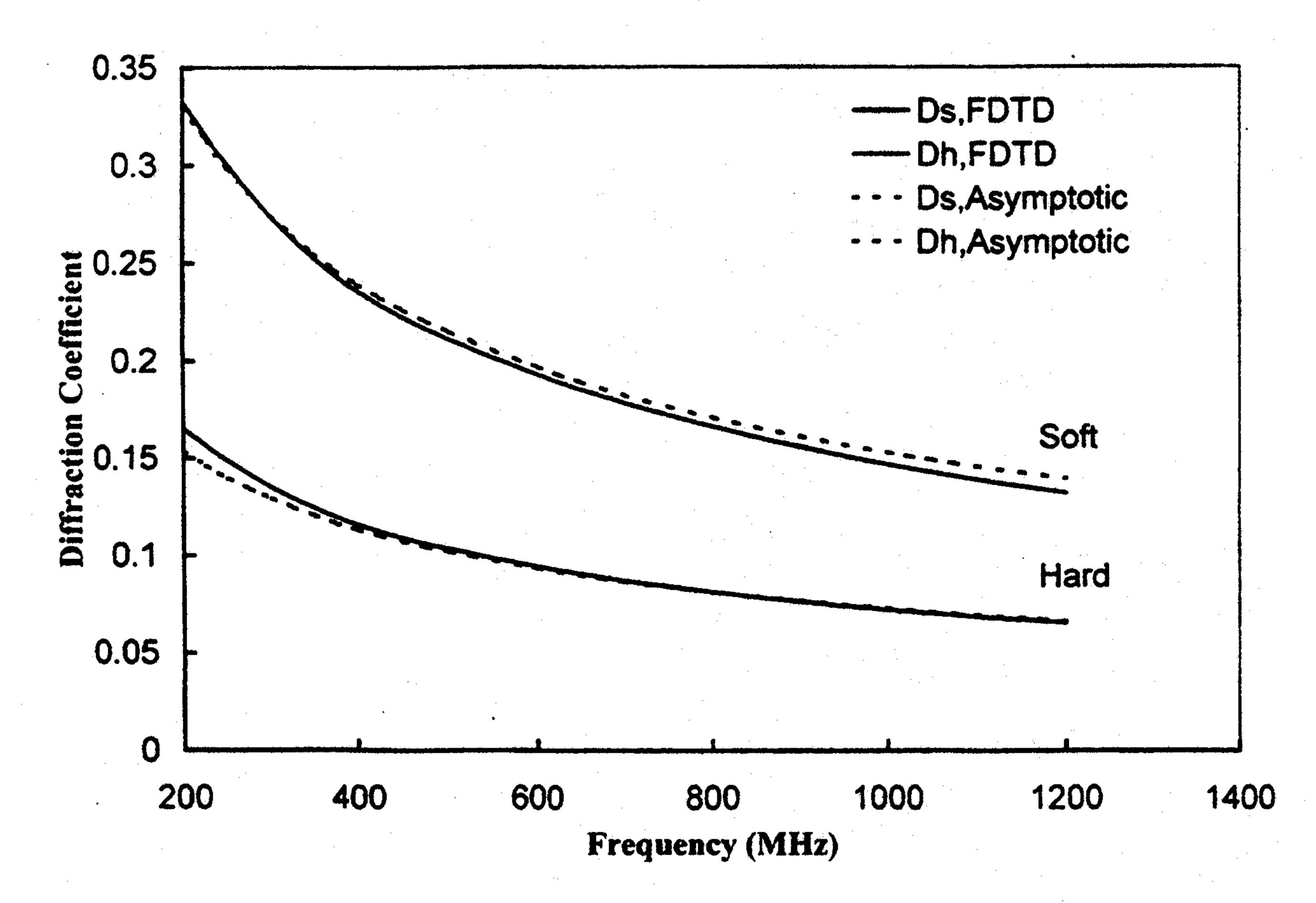


Fig. 2. Comparison of FDTD computed and asymptotic results for the soft and hard diffraction coefficients at a fixed observation point  $A_o(s=3\lambda_0,\phi=100^\circ,\beta_0=70^\circ)$  as a function of frequency for an obliquely incident plane wave at  $(\beta_0'=70^\circ,\phi'=150^\circ)$ .

and  $D_h$  can be calculated numerically as

$$D_{s,\text{FDTD}}(s,\theta,\phi,\omega) = H_{\beta_0,\text{num}}(s,\theta,\phi,\omega)\sqrt{s}e^{jk_0s} \qquad (1a)$$

$$D_{h,\text{FDTD}}(s,\theta,\phi,\omega) = H_{\phi,\text{num}}(s,\theta,\phi,\omega)\sqrt{s}e^{jk_0s} \qquad (1b)$$

where s is the distance of the observation point from the scattering edge and  $k_0 = \omega \sqrt{\mu_0 \varepsilon_0}$ . The Fourier transform has been defined using the  $e^{-j\omega t}$  convention. The factor,  $\sqrt{s}e^{jk_0s}$ , in the above equation arises from the nature of the Green's function in two dimensions.

Fig. 1 shows the 3-D geometry of the scatterer and the coordinate system used in the FDTD code. This figure also shows the edge-fixed spherical angles made by the incident ray  $(\beta'_0, \phi')$  and the diffracted ray  $(\beta_0, \phi)$ . Keller's law of edge diffraction implies that  $\beta'_0 = \beta_0$ . The unit vectors  $(\hat{\beta}'_0, \hat{\phi}')$  and  $(\hat{\beta}_0, \hat{\phi})$  are described in terms of the FDTD coordinate system  $(\hat{i}_f, \hat{j}_f, \hat{k}_f)$  using

$$\hat{\beta}_0' = -\cos\theta_f^i \cos\phi_f^i \hat{i}_f - \cos\theta_f^i \sin\phi_f^i \hat{j}_f + \sin\theta_f^i \hat{k}_f \qquad (2a)$$

$$\hat{\phi}' = -\sin\phi_f^i \hat{i}_f + \cos\phi_f^i \hat{j}_f \tag{2b}$$

$$\hat{\beta}_0 = \cos\theta_f^d \cos\phi_f^d \hat{i}_f + \cos\theta_f^d \sin\phi_f^d \hat{j}_f - \sin\theta_f^d \hat{k}_f \qquad (2c)$$

$$\hat{\phi} = \sin \phi_f^d \hat{i}_f - \cos \phi_f^d \hat{j}_f. \tag{2d}$$

Here, the angles  $(\theta_f^i, \phi_f^i)$  represent the direction of the incident plane wave illumination in the FDTD coordinate system. Further, the angles  $(\theta_f^d, \phi_f^d)$  represent the direction of the diffracted ray from the point of diffraction  $P_d$  to the observation point  $P_o$ . These angles can be easily derived from the edge-fixed angles using  $\theta_f^i = \theta_f^d = \beta_0$ ,  $\phi_f^i = \pi - \phi'$ , and  $\phi_f^d = 2\pi - \phi$ .

To minimize numerical errors in the FDTD code, we use cubic lattice cells of side length  $\lambda_0/25$ , where  $\lambda_0$  is the wavelength at 850 MHz and perfectly matched layer (PML) absorbing boundary condition. The incident illumination  $\vec{E}_{\rm inc}^{\rm num}$  is a pulsed plane wave of center frequency 850 MHz and a Gaussian envelope of 882.3-ps duration (full width at half maximum). The observation points and the side lengths of the scatterer are chosen such that the numerical diffraction field  $\vec{E}_{\rm dif}^{\rm num}$  from edge BC can be causally isolated in time from all the other fields. Using (1a) and (1b), the numerical diffraction coefficients are given by

$$D_{s,\text{FDTD}}(s,\theta_f^d,\phi_f^d,\omega) = \frac{\Im\{\vec{E}_{\text{dif}}^{\text{num}}(t,s,\theta_f^d,\phi_f^d)\cdot\hat{\beta}_0\}}{\Im\{\vec{E}_{\text{inc}}^{\text{num}}(t,\theta_f^i,\phi_f^i)\cdot\hat{\beta}_0'\}}\sqrt{s}e^{jk_0s}$$

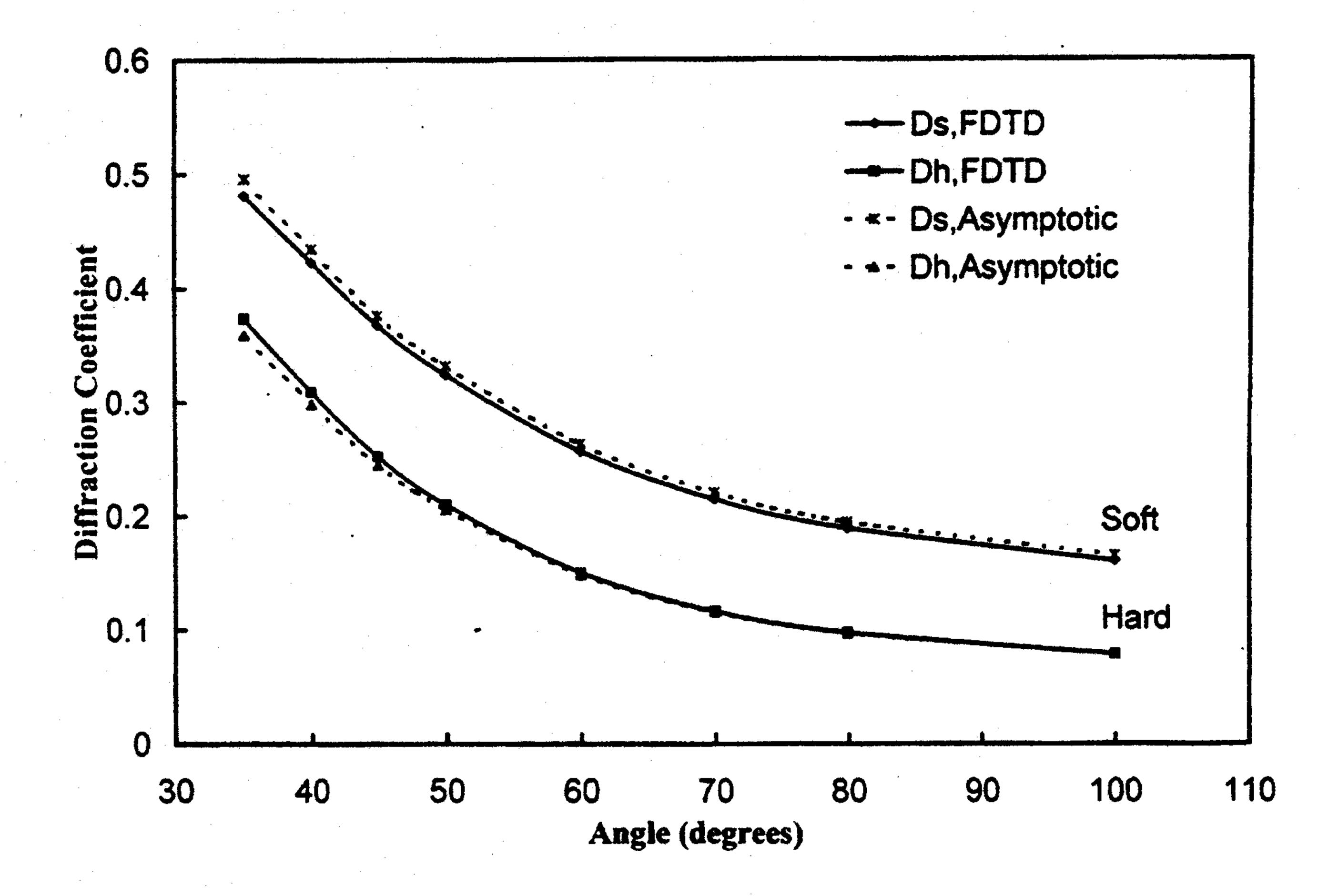


Fig. 3. Comparison of FDTD computed and asymptotic results for the soft and hard diffraction coefficients at 850 MHz as a function of the observation angle  $\phi$  at  $(\beta_0 = 70^\circ, s = 3\lambda_0)$  for an obliquely incident plane wave at  $(\beta_0' = 70^\circ, \phi' = 150^\circ)$ .

$$D_{h,\text{FDTD}}(s,\theta_f^d,\phi_f^d,\omega) = \frac{\Im\{\vec{E}_{\text{dif}}^{\text{num}}(t,s,\theta_f^d,\phi_f^d)\cdot\hat{\phi}\}}{\Im\{\vec{E}_{\text{inc}}^{\text{num}}(t,\theta_f^i,\phi_f^i)\cdot\hat{\phi}'\}}\sqrt{s}e^{jk_0s}$$
(3b)

where 3 denotes the Fourier transform operation.

Two cases are shown, comparing the amplitude of the FDTD computed dyadic diffraction coefficient of a PEC wedge to the wellknown asymptotic solution obtained using the uniform theory of diffraction (UTD) [1], [3]. For both cases, the plane wave illumination is assumed to be obliquely incident at  $(\beta'_0 = 70^{\circ}, \phi' = 150^{\circ})$ . Fig. 2 shows the variation of the amplitude of the soft and hard diffraction coefficients as a function of frequency at a fixed observation point  $A_o(s=3\lambda_0,\phi=100^\circ,\beta_0=70^\circ)$  over the frequency range 200 MHz to 1.2 GHz. Fig. 3 shows the variation of the amplitude of the soft and hard diffraction coefficients at the center frequency (850 MHz) as a function of the observation angle  $\phi$  at  $\beta_0 = 70^{\circ}$  and a fixed observation distance ( $s = 3\lambda_0$ ) from the point of diffraction  $P_d$ . Over the range of frequencies and observation angles considered in these figures, the worst-case difference between the FDTD and asymptotic results is only about 5%. Our numerical convergence studies indicate that the FDTD data are essentially converged at a space-cell size of  $\lambda_0/25$  for the cases under consideration.

## REFERENCES

- [1] G. Stratis, V. Anantha, and A. Taflove, "Numerical calculation of diffraction coefficients of generic conducting and dielectric wedges using FDTD," *IEEE Trans. Antennas Propagat.*, vol. 45, pp. 1525–29, Oct. 1997.
- [2] R. G. Kouyoumjian and P. H. Pathak, "A uniform geometrical theory of diffraction for an edge in perfectly conducting surface," *Proc. IEEE*, vol. 62, pp. 1448–1461, Nov. 1974.
- [3] C. A. Balanis, "Geometrical theory of diffraction," Advanced Engineering Electromagnetics. New York: Wiley, 1989, ch. 13.